

# INTERRUPTER SIZE EFFECT ON CURRENT ZERO PROPERTIES IN THERMAL INTERRUPTION OF HIGH VOLTAGE CIRCUIT BREAKERS

TOSHIAKI SAKUYAMA<sup>1\*</sup>, HAJIME URAI<sup>1</sup>, HIDEYUKI KOTSUJI<sup>1</sup>,  
NORIYUKI YAGINUMA<sup>1</sup>, MASANORI TSUKUSHI<sup>1</sup>

<sup>1</sup> Hitachi, Ltd., 316-8501, Hitachi, Japan  
\* toshiaki.sakuyama.cj@hitachi.com

## ABSTRACT

Current-zero measurements performed during interruption tests have been a powerful tool for measuring the thermal interruption performance of high-voltage gas circuit breakers. This performance is evaluated by estimating the extinction peak of arc voltage ( $V_p$ ) and/or arc conductance at 200 ns before current zero ( $G_{200}$ ). However, it is difficult to estimate the interruption performance for actual size circuit breakers. To investigate the size effect, the relationships between  $V_p$  and  $G_{200}$  for a small model and actual size model were compared. By introducing an interrupter size factor, we found that the boundary values of  $V_p$  and  $G_{200}$ , which distinguish the success and failure of interruption, corresponded with each other.

## 1. INTRODUCTION

Digital testing has been proposed to quantitatively evaluate the thermal interruption performance of circuit breakers with arc characteristics around current zero<sup>[1],[2]</sup>. Only a few pieces of data on arc characteristics that can be used to evaluate the performance of actual size interrupters are available. The authors have investigated the relationship between interruption performance and arc characteristics for small experimental models<sup>[3],[4]</sup>. It is necessary to clarify the effect of the size of interrupters to design an actual size interrupter by using experimental data obtained with a small model. The interruption performance and current zero data were measured for two different sized interrupters in this research. The relationship between interruption performance and arc characteristics, e.g., the extinction peak of arc voltage ( $V_p$ ) and arc conductance at 200 ns

before current zero ( $G_{200}$ ) calculated by using a current and voltage measured around current zero, was particularly investigated in terms of the interrupter size factor.

## 2. EXPERIMENTAL SETUP

### 2.1 Experimental circuit breaker

The interruption performance and current zero data were measured with two different size interrupters to investigate the effect of interrupter size on arc parameters. The interrupters were designed as pure self-blast types without mechanical puffer chambers for the experiment. Fig. 1 outlines a small model interrupter whose size is about half that of actual interrupters. The larger interrupters were sized up from the small model with the scale factors summarized in Table 1. Two different types of interrupter designed as the prototype for 50 kA (Type I) and 63 kA (Type II) rating were tested.

### 2.2 Experimental circuit for thermal interruption test

Fig. 2 is a circuit diagram for the current injection interruption test. The main interruption current was supplied from a current source with an inductance-capacitance (LC) resonance circuit. Current from the voltage source was injected just before the current zero of the main interruption current by operating the triggering gap. The main interruption current was set to 60 Hz or 35 Hz, depending on the test conditions, by changing the LC circuit parameters. The frequency of the main interruption current in tests for the small model interrupter was set at 35 Hz to interrupt the current zero at half cycle to make the test more efficient. The frequency of the first half cycle was set at 35 Hz for a large model interrupter and that of the second cycle was changed to 60 Hz.

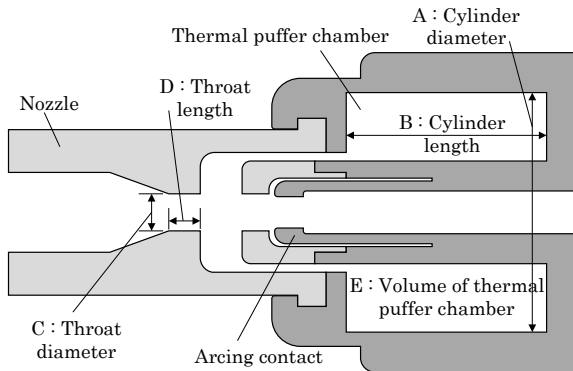


Fig. 1. Structure of small model interrupter

Table 1. Size coefficient of large interrupter for small interrupter (large/small)

	A	B	C	D	E
Type I	1.7	1.7	1.9	4.5	3.4
Type II	1.7 - 1.8	1.3 - 1.4	1.6	1.5 - 1.7	4.0 - 4.7

Thermal interruption performance can be determined within several microseconds just after current zero. The initial part of the transient recovery voltage (TRV) specified for 90% short-line fault (SLF) duty was applied to focus on evaluating thermal interruption in the current injection interruption test. The characteristic impedance was set at  $450 \Omega$  by adjusting  $R_f$ ,  $L_f$ , and  $C_f$ .

### 2.3 Current zero measurement system

The current zero measurement system consists of a data logger with 100-MHz sampling, a 14-bit resolution digitizing unit, and voltage and current measurement sensors, shown in Fig. 3. Voltage between the contacts was measured with high voltage probes. Both lower and higher side voltages were measured with two voltage probes. The temporal differentiation of current ( $di/dt$ ) was measured for the current by using a Rogowski coil.

## 3. RESULTS

Fig. 4 shows representative waveforms measured in the interruption test for the small model. The main interrupting current was 32 kArms, and the arcing time was 10.8 ms. Pressure in the thermal puffer chamber was measured with a piezo pressure gauge.

Fig. 5 shows representative waveforms measured in the interruption test for the large models. The frequency was changed from 35 Hz to 60 Hz at

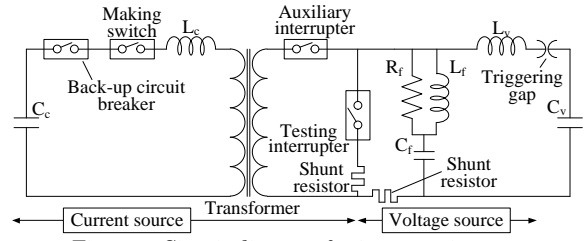


Fig. 2. Circuit diagram for interruption test

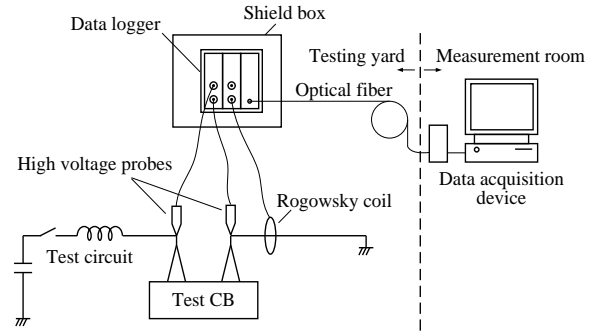


Fig. 3. Current zero measurement system

the first current zero point. The current value of the second half cycle was 45.9 kArms, and the arcing time was 18.3 ms. The peak of pressure in the thermal puffer chamber was almost equal to that of the small models.

Fig. 6 shows representative waveforms in the current zero measurements for the interruption test for the small model. Current waveform was calculated by digitally integrating the  $di/dt$  measured with the Rogowski coil. Arc conductance was also calculated from the arc voltage and current.

The thermal interruption performances of the small and large model interrupters were estimated by using the electrical properties around current zero. Fig. 7 plots the relationship between test results, namely, the success or failure of interruption and arc characteristics such as the extinction peak of the arc voltage ( $V_p$ ) and arc conductance at 200 ns before current zero ( $G_{200}$ ). As seen in the figure, a higher  $V_p$  and lower  $G_{200}$  are required to interrupt a higher  $di/dt$ . Therefore,  $V_p$  and  $G_{200}$  can serve as indicators to measure thermal interruption performance. For example, the  $V_p$  and  $G_{200}$  required to interrupt the L90 rating 50 kA - 60 Hz ( $di/dt = 24.0 \text{ A}/\mu\text{s}$ ) gas circuit breakers (GCBs) were more than 1.66 kV for the former and less than 3.95 mS for the latter as a result of interruption tests on the small model. In the same way, those for the large model were estimated to be more than 4.46 kV ( $V_p$ ) and less than 1.45 mS ( $G_{200}$ ), respectively.

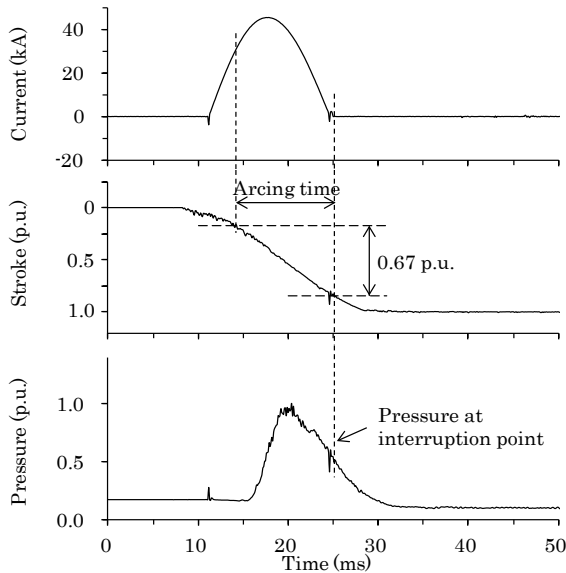


Fig. 4. Measured waveforms in test on small model interrupter

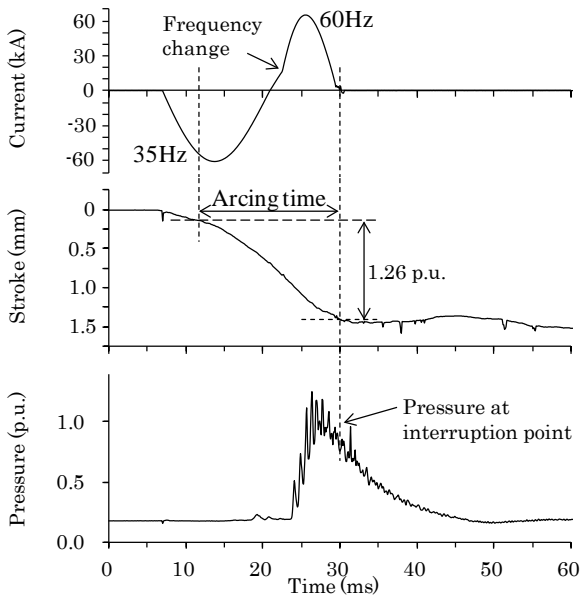


Fig. 5. Measured waveforms in test on large model interrupter

#### 4. DISCUSSION

Fig. 8 plots the correlation between  $V_p$  and  $G_{200}$ . The measured data for the  $di/dt$  around  $24.0 \text{ A}/\mu\text{s}$  are directly plotted in Fig. 8(a). As shown in this figure,  $G_{200}$  is proportional to the -1.66 power of  $V_p$ . The  $V_p$  was more than 1.5 kV, and  $G_{200}$  was less than 4.3 mS in the small model as the condition for successful interruption. The  $V_p$  was more than 4 kV, and  $G_{200}$  as less than 1.6 mS in the large model. The condition for successful interruption is different for the small and large models. These correlations can be converted with

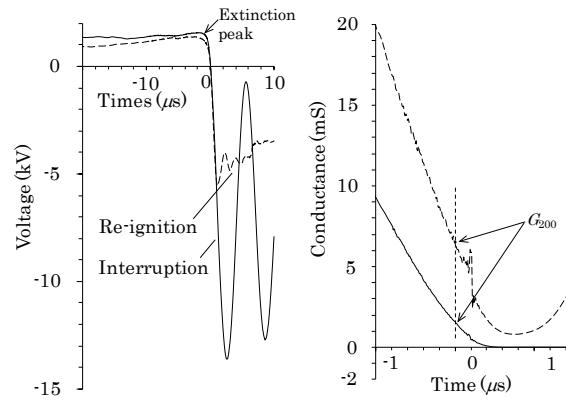


Fig. 6. Waveforms of arc voltage and conductance around current zero (small model)

the following method by taking into consideration the difference in interrupter sizes.

First, arc voltage ( $V_a$ ) and arc conductance ( $G_a$ ) are described as follows.

$$V_a = E_a \cdot L_a \dots\dots\dots (1)$$

$$G_a = \frac{I_a}{V_a} = \frac{I_a}{E_a L_a} \dots\dots\dots (2)$$

, where  $E_a$ ,  $L_a$ , and  $I_a$  correspond to voltage per unit length (arc potential gradient), arc length, and arc current.

The  $E_a$  is generally almost constant. The  $V_a$  is approximately proportional to  $L_a$ , and  $G_a$  is inversely proportional to  $L_a$ , which is proportional to the distance between arcing contacts. Thus,  $V_p$  and  $G_{200}$  are assumed to be described as coefficient  $k_L$ , which indicates the distance between arcing contacts as

$$V_p^* = k_L V_p \dots\dots\dots (3)$$

$$G_{200}^* = G_{200}/k_L \dots\dots\dots (4)$$

, where the superscripted asterisk (\*) indicates the value converted from the large to the small model. Coefficient  $k_L$  for rating 50 kA – 60 Hz is calculated with the approximate curve in Fig. 8(a) as

$$k_L = \left( \frac{16.1}{8.6} \right)^{\frac{1}{0.66}} = 2.59 \dots\dots\dots (5)$$

In the same way, the  $k_L$  for rating 63 kA – 60 Hz was calculated to be 1.40. The results for the small model tests converted with  $k_L$  are plotted in Fig. 8(b) and Fig. 8(c). The boundary values that distinguish the success and failure of interruption for both models agreed well. However,  $k_L$  was different from the ratio of each distance between arcing contacts. The ratio was 1.88, calculated from the arcing contact distance at current zero point in Figs. 5 and 6. This implies that not only

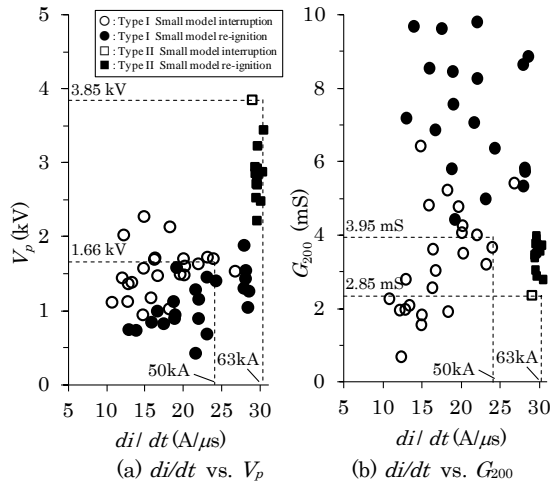


Fig. 7. Example of measurement characteristics (small model interrupters)

arc length but also other size parameters should be considered, which is an issue to be addressed in the future.

## 5. CONCLUSION

Interruption tests were carried out, and current and voltage were measured with a system to measure current zero for two different size interrupters to investigate the effect of size and evaluate the performance of parameters such as the extinction peak of arc voltage and arc conductance. As a result, we found that the boundary values of  $V_p$  and  $G_{200}$  corresponded to the distinguished success and failure of interruption by introducing an interrupter size factor.

## REFERENCES

- [1] René Peter Paul Smeets, Viktor Kertész, Susumu Nishiwaki, and Katsumi Suzuki, "Performance Evaluation of High-Voltage Circuit Breakers by Means of Current Zero Analysis", Proceedings of IEEE/PES Transmission and Distribution Conference, Vol. 1, pp. 424 - 429, 2002.
- [2] R. P. P. Smeets, V. Kertész, H. Knobloch, U. Habedank, A. Even, P. Scarpa, C. Neumann, B. Krampe, L. van der Sluis, and P. Schavemaker, "Digital Testing of High-Voltage Circuit Breakers", ELECTRA, No. 204, pp. 20 - 29, 2002.
- [3] Hajime Urai, Yoichi Ooshita, Makoto Koizumi, and Masanori Tsukushi, "Evaluation of arc extinction performance with arc conductance at current-zero in a gas circuit breaker", Papers of Joint Technical Meeting on Electrical Discharges, Static Apparatus and Switching and Protecting Engineering, IEE Japan, ED-07-120, SA-07-52, SP-07-77, 2007 (in Japanese).
- [4] Hajime Urai, Yoichi Ooshita, Makoto Koizumi, and Masanori Tsukushi, "Evaluation of Thermal Interruption Capability in SF6 Gas Circuit Breakers with Re-ignition Voltage and its Application to Experimental Design", IEEJ Transactions on Power and Energy, Vol. 132, No. 5, pp. 407 - 414, 2012.

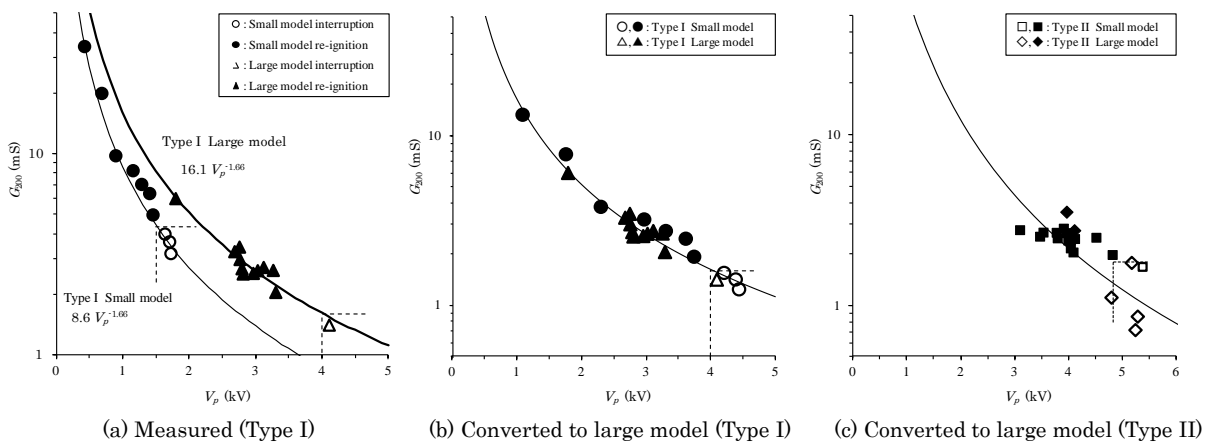


Fig. 8. Relationship between  $V_p$  and  $G_{200}$